International Conference on Textile Composites and Inflatable Structures
STRUCTURAL MEMBRANES 2011
E. Oñate, B. Kröplin and K.-U.Bletzinger (Eds)

PRESSURE-VOLUME COUPLING IN INFLATABLE STRUCTURES

Marianna Coelho*, Kai-Uwe Bletzinger* and Deane Roehl†

*Technische Universität München (CIMNE)
Lehrstuhl für Statik
Arcisstr. 21, 80333 Munich, Germany
e-mail: coelho@bv.tu-muenchen.de, kub@bv.tu-muenchen.de

†Pontifícia Universidade Católica do Rio de Janeiro (PUC-Rio)
Department of Civil Engineering
Rua Marques de Sao Vicente 225, 22451-900 Rio de Janeiro, Brazil
e-mail: droehl@puc-rio.br

Key words: Deformation-dependent forces, Inflatable structures, Pressure-volume coupling, Multi-chambers, Membrane finite element

Abstract. Inflatable structures or pneumatic structures are air-supported structures and find application in a variety of new engineering projects. By these structures the gas gives shape and strength to the structure in such a way that with larger volumes and higher pressures larger spans can be abridged. Their architectonic flexibility and the search for better structural efficiency are strong favorable arguments to the use of this kind of structure. Furthermore, inflatable structures can be erected or dismantled quickly, are light, portable and materially inexpensive. Also, some characteristics such as the utilization of natural lighting and ventilation and its possibility of reuse contribute to the pursuit of sustainable development. In this work the influence of the pressure-volume coupling on structure behavior is studied. A membrane formulation with deformation-dependent forces was implemented in a finite element model to take into account the influence of gas volume variation, with corresponding change in pressure for enclosed gas on the stiffness of membrane structures. An analytical solution of inflatable membranes was developed for the validation of the numerical results. Comparisons are carried out on a clamped circular membrane inflated by a uniform pressure.

1 INTRODUCTION

Inflatable structures or pneumatic structures are according to Dent [6] structures acted on by air or gases and relate particularly to architecture and construction. Membrane foils are used in these structures and it is defined according to Pauletti[5] as a construc-

tive element in tension-structures that balance the external loads with tensile and shear stresses tangent to the structure surface. Otto[14, 13] defines a membrane as a flexible skin stretched in such a way to be subjected to tension. The membrane finite element formulation used is described in the works of Wüchner and Bletzinger [18], Vázquez [17] and Linhard [12].

The properties and the different shapes of pneumatic structures is described in the work of Herzog [10]. A large number of parameters determine the final shape of these structures: type of internal pressure, magnitude of internal pressure, boundary conditions, number of membranes, type of utilization, membrane material, surface curvature, etc.

The pressure-volume coupling will be considered in the analyses of the pneumatic structure. The numerical implementations of the finite element coupling model was carried out on the program used in the Static Chair at TUM (Technische Universität München). This program is called CARAT++ (Computer Aided Research Analysis Tool) and it has been started by Kai-Uwe Bletzinger, Hans Stegmüller and Stefan Kimmich at the Institut für Baustatik of the University of Stuttgart in 1987. In accordance with its title, CARAT served first of all as a research code.

An analytical solution of inflatable membranes for the validation of the numerical results was developed. The results for the analytical and numerical analysis clarify the influence of the pressure-volume coupling and highlight the importance to consider this coupling in these type of structure.

2 DEFORMATION-DEPENDENT FORCES

The objective to implement the pressure-volume coupling is to take into account influences of gas volume variation, which leads to the change in pressure for an enclosed gas on the stiffness of membrane structures. According to Jarasjarungkiat ([11]) numerical examples demonstrate not only the efficiency of the model but also the need to consider the volume (pressure) variation in addition to the change of surface normal vector. This work reveals the observable feature that the pressure of an enclosed fluid provides additional stiffness to the inflatable structure, analogous to the behavior of a membrane on elastic springs.

For this implementation the concept of deformation-dependent forces was studied. The formulation used within this work refers to the works of Hassler and Schweizerhof [9], Rumpel and Schweizerhof [16], Rumpel [15], Bonet et. ali. [2] and Berry and Yang [1].

Hassler and Schweizerhof [9] presented a formulation for the static interaction of fluid and gas for large deformation in finite element analysis that can be applied to pneumatic structures. Moreover it provides a realistic and general description of the interaction of arbitrarily combined fluid and/or gas loaded or filled multi-chamber systems undergoing large deformations static or quasi-static .

The use of a deformation-dependent force formulation brings along the drawback of a fully-populated stiffness matrix whose triangular factorization requires large numerical effort. To circumvent this problem Woodbury's formula was used to solve the fully-

populated stiffness matrix as discussed in the work of Hager [8]. The Woodbury's formula updates the inverse of a matrix with the update tensors without performing a new factorization of the stiffness matrix.

2.1 Numerical analysis model

The formulation presented in the work of Hassler and Schweizerhof [9] concern an enclosed volume filled with combined fluid and gas. Rumpel and Schweizerhof [16] treat the case of structures filled with gas, which is the common case in civil engineering. Therefore, the formulation considered in this work concern an enclosed volume filled with gas. This formulation will be briefly present:

Taking the principle of virtual work as basis for the problem formulation, the external virtual work of a pressure load is given by:

$$\delta\Pi_{press} = \int_a p\,\mathbf{n}\cdot\delta\mathbf{u}\,da \tag{1}$$

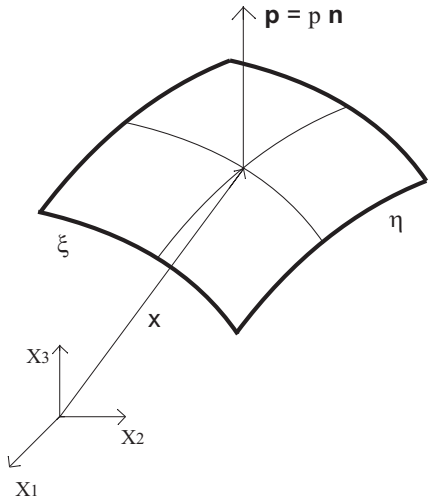

Figure 1: Surface under pressure loading.

where $\mathbf{n} = \mathbf{x}_{,\xi} \times \mathbf{x}_{,\eta} / |\mathbf{x}_{,\xi} \times \mathbf{x}_{,\eta}|$ is the normal, $da = |\mathbf{x}_{,\xi} \times \mathbf{x}_{,\eta}|\, d\xi d\eta$ is the surface element and $p = p(v(\mathbf{x}))$ is the internal pressure. The surface vector $\mathbf{x}(\xi, \eta)$ depends on local co-ordinates ξ and η represented in Figure 1. Substitution of the definition 1 gives:

$$\begin{aligned}\delta\Pi_{press} = \int_\eta \int_\xi p \frac{\mathbf{x}_{,\xi} \times \mathbf{x}_{,\eta}}{|\mathbf{x}_{,\xi} \times \mathbf{x}_{,\eta}|} \cdot \delta\mathbf{u}\ |\mathbf{x}_{,\xi} \times \mathbf{x}_{,\eta}|\, d\xi d\eta \ &= \int_\eta \int_\xi p\,(\mathbf{x}_{,\xi} \times \mathbf{x}_{,\eta})\, d\xi d\eta \\ &= \int_\eta \int_\xi p\,\mathbf{n}^* \cdot \delta\mathbf{u}\, d\xi d\eta\end{aligned} \tag{2}$$

According to Poisson's law, the constitutive behavior of the gas is describe by the following equation:

$$pv^{\kappa} = PV^{\kappa} = const \tag{3}$$

where κ is the isentropy constant, P and V are the initial pressure and volume for a closed chamber. This equation demonstrates that the final pressure is inversely proportional to the final volume, in other words, when the volume decreases the internal pressure inside the enclosed volume will increase.

When $\kappa = 1$ the adiabatic change simplifies to Boyle's law.

The volume for the enclosed chamber v is computed through the equation:

$$v = \frac{1}{3}\int_{\eta}\int_{\xi} \mathbf{x}\cdot\mathbf{n}^{*}\, d\xi d\eta \tag{4}$$

The external virtual work is linearized for the solution with a Newton scheme. Equation 2 and the constraint 3 are expanded into a Taylor series up to the first order term:

$$\delta\Pi^{lin}_{press} = \delta\Pi_{press} + \delta\Pi^{\Delta p}_{press} + \delta\Pi^{\Delta \mathbf{n}}_{press} \tag{5}$$

$$\delta\Pi^{lin}_{press} = \int_{\eta}\int_{\xi} (p\mathbf{n}^{*}\cdot\delta\mathbf{u} + \Delta p\mathbf{n}^{*}\cdot\delta\mathbf{n}^{*} + p\Delta\mathbf{n}^{*}\cdot\delta\mathbf{u})\, d\xi d\eta$$

with

$$\Delta\mathbf{n}^{*} = \Delta\mathbf{u}_{,\xi}\times\mathbf{x}_{,\eta} - \Delta\mathbf{u}_{,\eta}\times\mathbf{x}_{,\xi} \tag{6}$$

$$\Delta(pv^{\kappa}) = 0 \quad , \; pv^{\kappa} = constant \tag{7}$$
$$\Delta p\cdot v^{\kappa} + \Delta v^{\kappa}\cdot p = 0$$

where

$$\Delta v^{\kappa} = \kappa\frac{v^{\kappa}}{v}\Delta v \tag{8}$$

$$\Delta v = \frac{1}{3}\int_{\eta}\int_{\xi} [\Delta\mathbf{u}\cdot\mathbf{n}^{*} + \mathbf{x}\cdot\Delta\mathbf{n}^{*}]\, d\xi d\eta = \Delta v^{\Delta\mathbf{u}} + \Delta v^{\Delta\mathbf{n}} \tag{9}$$

Equation 7 results in:

$$\Delta p + \frac{\kappa p}{v}\Delta v = 0 \tag{10}$$

In this work the final results for the partial integrations of equation 5 will be presented. The solution for each part of the partial integration of the external virtual work is shown in References [9], [16] and [15]. The partial integration of the external virtual work due to the change in the normal vector is given by:

$$\delta\Pi^{\Delta\mathbf{n}}_{press} = \frac{p}{2}\int_{\eta}\int_{\xi} \begin{pmatrix} \delta\mathbf{u} \\ \delta\mathbf{u}_{,\xi} \\ \delta\mathbf{u}_{,\eta} \end{pmatrix} \cdot \begin{bmatrix} 0 & \underline{\mathbf{W}}^{\xi} & \underline{\mathbf{W}}^{\eta} \\ \underline{\mathbf{W}}^{\xi T} & 0 & 0 \\ \underline{\mathbf{W}}^{\eta T} & 0 & 0 \end{bmatrix} \begin{pmatrix} \Delta\mathbf{u} \\ \Delta\mathbf{u}_{,\xi} \\ \Delta\mathbf{u}_{,\eta} \end{pmatrix} d\xi d\eta \tag{11}$$

The partial integration of the external virtual work due to the change in the pressure is:

$$\delta\Pi_{press}^{\Delta p} = -\frac{\kappa p}{v}\int_\eta\int_\xi \mathbf{n}^* \cdot \Delta\mathbf{u}\, d\xi d\eta \int_\eta\int_\xi \mathbf{n}^* \cdot \delta\mathbf{u}\, d\xi d\eta \tag{12}$$

Replacing equations 11 and 12 in equation 5 gives:

$$\begin{aligned} \delta\Pi_{press}^{lin} = 0 \qquad \delta\Pi_{press}^{\Delta p} + \delta\Pi_{press}^{\Delta \mathbf{n}} &= -\delta\Pi_{press} \\ -\frac{\kappa p}{v}\int_\eta\int_\xi \mathbf{n}^* \cdot \Delta\mathbf{u}\, d\xi d\eta \int_\eta\int_\xi \mathbf{n}^* \cdot \delta\mathbf{u}\, d\xi d\eta & \\ +\frac{p}{2}\int_\eta\int_\xi \begin{pmatrix} \delta\mathbf{u} \\ \delta\mathbf{u}_{,\xi} \\ \delta\mathbf{u}_{,\eta} \end{pmatrix} \cdot \begin{bmatrix} 0 & \underline{\mathbf{W}}^{\xi} & \underline{\mathbf{W}}^{\eta} \\ \underline{\mathbf{W}}^{\xi T} & 0 & 0 \\ \underline{\mathbf{W}}^{\eta T} & 0 & 0 \end{bmatrix} \begin{pmatrix} \Delta\mathbf{u} \\ \Delta\mathbf{u}_{,\xi} \\ \Delta\mathbf{u}_{,\eta} \end{pmatrix} d\xi d\eta & \\ = -p\int_\eta\int_\xi \mathbf{n}^* \cdot \delta\mathbf{u}\, d\xi d\eta & \end{aligned} \tag{13}$$

The discretization for the finite element is applied taking the equations 13 and the isoparametric representation:

$$\mathbf{x} = \mathbf{N}\mathbf{x}, \qquad \Delta\mathbf{u} = \mathbf{N}\mathbf{d} \quad \textit{and} \quad \delta\mathbf{u} = \mathbf{N}\delta\mathbf{d} \tag{14}$$

The global stiffness matrix and the global load vector are given:

$$\left[\mathbf{K}_T - (\mathbf{K}_{press} - b\mathbf{a}\otimes\mathbf{a})\right]\mathbf{d} = \mathbf{f}_{ext} + \mathbf{f}_{press} - \mathbf{f}_{int} \tag{15}$$

$$\mathbf{K}_{press} = \frac{p}{2}\int_\eta\int_\xi \begin{pmatrix} \delta\mathbf{N} \\ \delta\mathbf{N}_{,\xi} \\ \delta\mathbf{N}_{,\eta} \end{pmatrix}^T \cdot \begin{bmatrix} 0 & \underline{\mathbf{W}}^{\xi} & \underline{\mathbf{W}}^{\eta} \\ \underline{\mathbf{W}}^{\xi T} & 0 & 0 \\ \underline{\mathbf{W}}^{\eta T} & 0 & 0 \end{bmatrix} \begin{pmatrix} \Delta\mathbf{N} \\ \Delta\mathbf{N}_{,\xi} \\ \Delta\mathbf{N}_{,\eta} \end{pmatrix} d\xi d\eta \tag{16}$$

$$\mathbf{a} = \int_\eta\int_\xi \mathbf{N}^T\mathbf{n}^*\, d\xi d\eta \tag{17}$$

$$\mathbf{f}_{press} = p\int_\eta\int_\xi \mathbf{N}^T\mathbf{n}^*\, d\xi d\eta \tag{18}$$

$$b = \kappa\frac{p}{v} \tag{19}$$

where $\mathbf{K}_T$ is the stiffness matrix containing linear and non-linear terms, $\mathbf{K}_{press}$ is the load stiffness matrix for each structural element in contact with gas, $\mathbf{a}$ is the coupling vector, $\mathbf{f}_{press}$ is the load vector, $\mathbf{f}_{int}$ is the residuum vector and $\mathbf{f}_{ext}$ is the vector of the external forces. According Rumpel [15] the load stiffness matrix $\mathbf{K}_{press}$ reflect the direction

dependent of the internal pressure and the fully-populated coupling matrix $b\mathbf{a} \otimes \mathbf{a}$ is the volume dependent of the internal pressure.

Equation 15 can be rewritten as:

$$[\mathbf{K}^* + b\mathbf{a} \otimes \mathbf{a}]\,\mathbf{d} = \mathbf{F} \tag{20}$$

where $\mathbf{K}^* = \mathbf{K}_T - \mathbf{K}_{press}$ and $\mathbf{F} = \mathbf{f}_{ext} + \mathbf{f}_{press} - \mathbf{f}_{int}$.

The stiffness matrix is fully-populated, and therefore triangular factorization requires for its great computational effort. To circumvent this problem Woodbury's formula was used to solve the fully-populated stiffness matrix, as discussed in the work of Hager [8]. The Woodbury's formula updates the inverse of a matrix through the update tensors dismissing factorization of the stiffness matrix.

3 ANALYTICAL ANALYSIS

To perform an analytical analysis, circular inflated membrane clamped at its rim is inflated by a uniform pressure. The membrane is supposed to have large displacements, we refer to works from Hencky (see [7]), Fichter [7], Campbell [4] and Bouzidi et. ali. [3]. Fichter [7] considered that the lateral stress for this problem has a radial component. This radial component is neglected in Hencky's problem. Note that, Fichter and Hencky consider the membrane without initial tension. Campbell [4] generalized Hencky's problem to include the influence of an arbitrary initial tension.

In this work an analytical solution was developed for inflated circular membranes considering the radial component in the lateral stress and an arbitrary initial tension in the membrane.

3.1 Hencky's solution

Hencky's solution consider an uniform lateral loading, in other words, the radial component of pressure on the deformed membrane is neglected. The equation for radial equilibrium is:

$$N_\theta = \frac{d}{dr}(r \cdot N_r) \tag{21}$$

and for lateral equilibrium:

$$N_r \frac{d}{dr}(w) = -\frac{pr}{2} \tag{22}$$

where N_r and N_θ are the radial and circumferential stress resultants, respectively, r is the radial coordinate, w is the lateral deflection, and p is the uniform lateral loading. It is assumed that the material is linear and it has elastic behavior, then the stress-strain relations are:

$$N_\theta - \nu \cdot N_r = E \cdot h \cdot \epsilon_\theta \tag{23}$$

$$N_r - \nu \cdot N_\theta = E \cdot h \cdot \epsilon_r \tag{24}$$

The strain-displacement relation is given by:

$$\epsilon_r = \frac{d}{dr}(u) + \frac{1}{2} \cdot \left(\frac{dw}{dr}\right)^2 \tag{25}$$

$$\epsilon_\theta = \frac{u}{r} \tag{26}$$

where u is the radial displacement and μ is Poisson's ratio.

3.2 Fichter's solution

The equation of the radial equilibrium for Fichter's solution has, in comparison with the Hencky's solution (see equation 21), an addition term:

$$N_\theta = \frac{d}{dr}(r \cdot N_r) - p \cdot r\frac{w}{dr}(w) \tag{27}$$

This additional term comes from the normal pressure which is neglected in Hencky's solution. The equations of Fichter's solution for the lateral equilibrium and the stress-strain relation remain the same as those of Hencky's solution (see equations 22 through 26).

4 RESULTS

A circular membrane clamped at its rim is inflated by a uniform pressure. The membrane is assumed to have large deflection and small strain for the analytical and numerical solutions. The large strain is assumed just in the numerical solution because it is not available in the literature an analytical solution with large strain. The data used for the

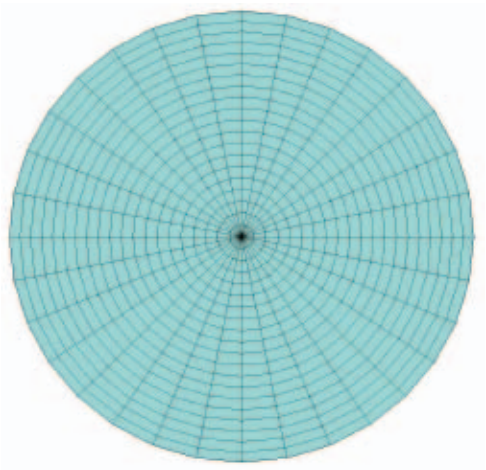

Figure 2: Mesh for a circular inflated membrane.

numerical and analytical analysis is from the work of Bouzidi et. ali. [3]. The membrane characteristics are: $E = 311488Pa.m$ (Young's modulus), $\nu = 0.34$ (Poisson ratio) and the radius is 0.1425 m. The static analysis was carried out in two steps. Initially the configuration for an internal pressure of 400kPa is obtained. After the inflation external pressures were applied. The mesh for the numerical solution is composed of 641 nodes and 640 membrane elements (see Figure 2). The membrane element has 4 nodes and 4 gauss integration points. It is also considered the plane stress state for the membrane element.

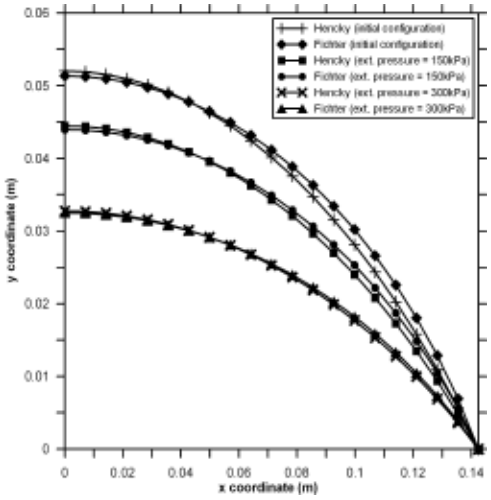

Figure 3: Comparison between the Hencky's and Fichter's solution for the applied external pressure of 150kPa and 300kPa.

In Figure 3 the results of Hencky's and Fichter's solution for the applied external pressure of 150kPa and 300kPa are presented. The difference between both solutions is due to the additional term present only in Fichter's solution associated to the normal pressure. The analytical solution from Fichter is closer to the solutions from numerical and experimental analysis. This can be observed in the Figure 4, which presents the results for the analytical and numerical solution due to the applied external pressure of 150kPa and 300kPa. The difference result obtained with Fichter's solution and the numerical solution is accredited to the presence of finite strains, which are included in the finite element formulation and are precluded in the analytical solution. In equation 28 the strain components with the finite strain contribution are shown.

$$\epsilon_r = \frac{du}{dr} + \frac{1}{2} \cdot \left(\frac{dw}{dr}\right)^2 + \frac{1}{2} \cdot \left(\frac{du}{dr}\right)^2 \qquad (28)$$

$$\epsilon_\theta = \frac{u}{r} + \frac{1}{2} \cdot \left(\frac{u}{r}\right)^2$$

The terms $\frac{du}{dr}$ and $\frac{u}{r}$ are the small strain, the term $\frac{1}{2} \cdot \left(\frac{dw}{dr}\right)^2$ arises in the presence of large

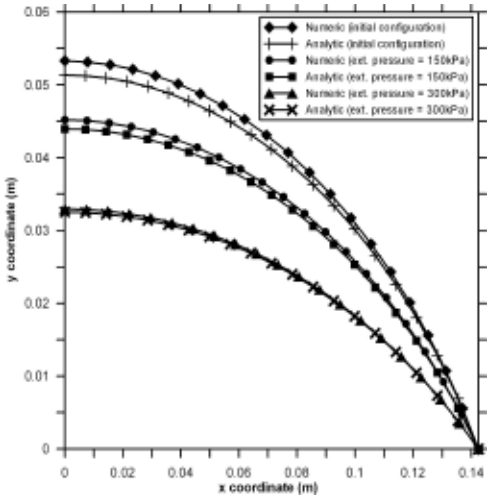

Figure 4: Result for the analytical and numerical solution without pretension and $\kappa = 0$ due to the applied external pressure of 150kPa and 300kPa.

displacements and the terms $\frac{1}{2} \cdot \left(\frac{du}{dr}\right)^2$ and $\frac{1}{2} \cdot \left(\frac{u}{r}\right)^2$ account for the finite strains.

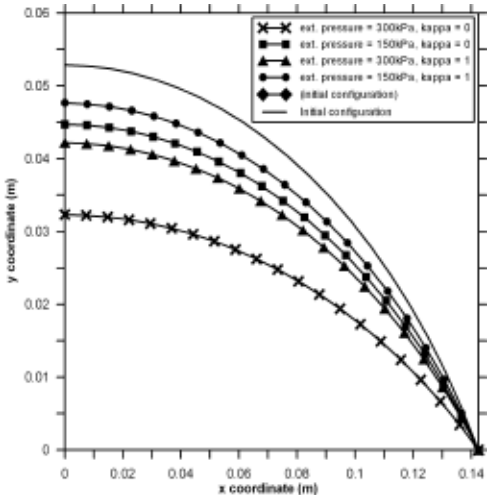

Figure 5: Comparison between the numerical solution with a pretension of 1kPa for $\kappa = 0$ and 1 due to the applied external pressure of 150kPa and 300kPa.

Figure 5 presents the result of a numerical solution for the circular membrane with pressure-volume coupling ($\kappa = 1$) and the case without the pressure-volume coupling ($\kappa = 0$). It is observed that the pressure-volume coupling is more noticeable for higher external pressure, in agreement with Poisson's law (see equation 3). It is important to observe according to the amount of coupling that different final configurations are obtained.

Next, the influence of pretension is investigated. In Figure 6 the results for the analyt-

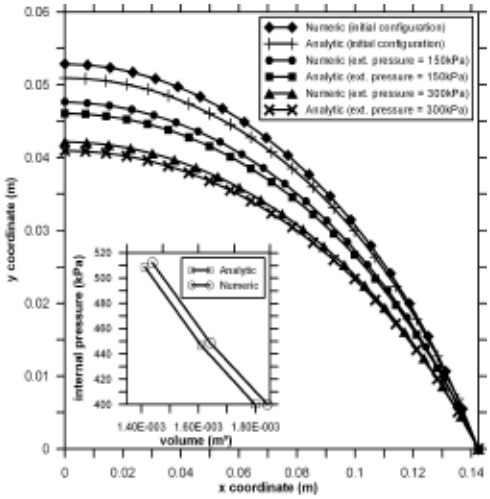

Figure 6: Result for the analytical and numerical solution with pretension of 1kPa and $\kappa = 1$ due to the applied external pressure of 150kPa and 300kPa.

ical and numerical solution with pretension of 1kPa and with pressure-volume coupling subjected to external pressures of 150kPa and 300kPa are presented . The analytical solution considers both the term from the normal pressure, which is neglected in Hencky's solution, and an initial tension, which is not considered in the Hencky's and Fichter's solution. It is observed that the results obtained with the analytical solution are in accordance with the numerical results. The relation between the internal pressure versus volume are illustrated in Figure 6, stressing that when the volume decreases due to the external pressure the internal pressure increase.

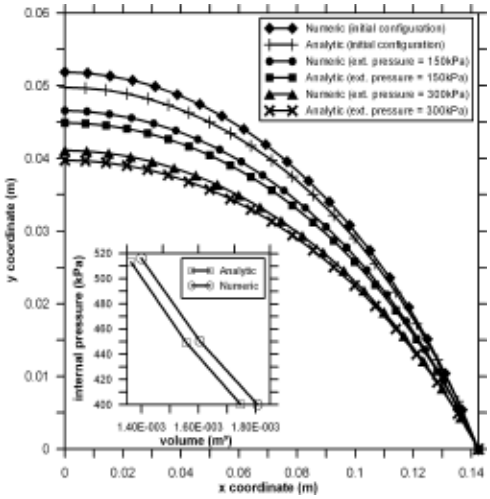

Figure 7: Result for the analytical and numerical solution with pretension of 4kPa and $\kappa = 1$ due to the applied external pressure of 150kPa and 300kPa.

In Figure 7 results for analytical and numerical solution with pretension of 4kPa and with pressure-volume coupling subjected to external pressures of 150kPa and 300kPa are presented. It is observed, comparing the results from Figures 7 and 6, that the deformed configuration and consequently the volume of the circular membrane decrease for the case with the pretension of 4kPa. Although the increase in the pretension is 4 times more, the decrease in the volume is not large. It can be observed in the graphics internal pressure versus volume in the Figures 7 and 6.

5 CONCLUSIONS

The present work analyzed pressure-volume coupling for a circular inflated membrane clamped at its rim. The results for the circular inflated membrane obtained with the analytical solution are in good accordance with the numerical solution. The pressure-volume coupling for the pneumatic structures was compared with the case when this coupling is not considered. It was shown that the final configuration with the coupling for the static analysis is very different in comparison with the analysis without this coupling, as defined by Poisson's law. It is also highlighted that higher external forces lead to higher internal pressure, due to the change in the configuration of the structure resulting in a decrease in the volume.

REFERENCES

[1] Dale T. Berry and Henry T. Y. Yang. Formulation and experimental verification of a pneumatic finite element. *International Journal for Numerical Methods in Engineering*, 39:1097–1114, 1996.

[2] J. Bonet and J. Mahaney. Form finding of membrane structures by the updated reference method with minimum mesh distortion. *International Journal of Solids and Structures*, 38:5469–5480, 2001.

[3] Rabah Bouzidi, Yannick Ravaut, and Christian Wielgosz. Finite elements for 2d problems of pressurized membranes. *Computer and Structures*, 81:2479–2490, 2003.

[4] J. D. Campbell. On the theory of initially tensioned circular membranes subjected to uniform pressure. *Quart. Journ. Mech. and Applied Math.*, 9:84–93, 1956.

[5] Ruy Marcelo de Oliveira Pauletti. *História, análise e projeto de estruturas retesadas*. Tese de livre docencia, Escola Politécnica da Universidade de São Paulo, São Paulo, 2003.

[6] Roger N. Dent. *Pneumatic Structures*. The Architectural Press, 1972.

[7] W. B. Fichter. Some solutions for the large deflections of uniformly loaded circular membranes. Technical report, Nasa Technical Paper 3658, Langley Research Center, Hampton, VA 23681-2199, July 1997.

[8] William W. Hager. Updating the inverse of a matrix. *Society for Industrial and Applied Mathematics*, 31:221–239, 1989.

[9] M. Hassler and K. Schweizerhof. On the static interaction of fluid and gas loaded multi-chamber systems in large deformation finite element analysis. *Computer methods in applied mechanics and engineering*, 197:1725–1749, 2008.

[10] T. Herzog. *Pneumatische Konstruktionen*. Stuttgart, 1976.

[11] Amphon Jarasjarungkiat. *Computational Mechanics of Pneumatic Membrane Structures: From Subgrid to Interface*. PhD thesis, Technische Universität München, 2009.

[12] Johannes Linhard. *Numerish-mechanische Betrachtung des Entwurfsprozesses von Membrantragwerken*. PhD thesis, Technischen Universität München, Fakultät für Bauingenieur- und Vermessungswesen, 2009.

[13] Frei Otto. *Tensile Structures - Cable Structures*, volume 2. The M.I.T. Press, 1st edition, 1969.

[14] Frei Otto. *Tensile Structures - Pneumatic Structures*, volume 1. The M.I.T. Press, 1st edition, 1969.

[15] T. Rumpel. *Effiziente Diskretisierung von statischen Fluid-Struktur-Problemen bei grossen Deformationen*. PhD thesis, Fakultät für Maschinenbau der Universität Karlsruhe (TH), 2003.

[16] T. Rumpel and K. Schweizerhof. Volume-dependent pressure loading and its influence on the stability of structures. *International Journal for Numerical Methods in Engineering*, 56:211–238, 2003.

[17] Jésus Gerardo Valdés Vázquez. *Nonlinear Analysis of Orthotropic Membrane and Shell Structures Including Fluid-Structure Interaction*. PhD thesis, Universitat Politécnica de Catalunya, 2007.

[18] R. Wüchner and K.-U. Bletzinger. Stress-adapted numerical form finding of prestressed surfaces by the updated reference strategy. *International journal for numerical methods in engineering*, 64(2):143–166, 2005.